JOURNAL OF AIRCRAFT
Vol. 44, No. 3, May–June 2007

Effect of Oscillation on Boundary-Layer Development with Adverse Pressure Gradients

K. Kontis* and M. Amir†
University of Manchester, Manchester, M60 1QD England, United Kingdom

DOI: 10.2514/1.25450

An experimental study has been conducted to investigate the effects of oscillation, of varying amplitude (0 to 0.03 m) and frequency (0 to 6 Hz), on the boundary-layer development of a flat plate under the influence of adverse pressure gradients. The Reynolds number was 10^6 based on the flat plate chord length. The study employed a subsonic wind tunnel facility at a freestream velocity of 16 m/s. A cylinder placed at various locations over the flat plate within the boundary layer was used to create the effects of adverse pressure gradients. Surface pressures were measured along the centerline of the flat plate to study the flow quantitatively. Oil flow visualizations were also obtained to examine the flow qualitatively. Boundary-layer surveys were conducted to examine the effect of oscillation on the mean velocity, turbulence intensity, and boundary-layer thickness profiles.

Nomenclature

A	=	amplitude of oscillation
D	=	cylinder diameter
F	=	frequency of oscillation
ℓ	=	length of the flat plate
P	=	local static pressure
P_∞	=	freestream static pressure
Re_{crit}	=	critical Reynolds number
Re_N	=	Reynolds number
S_t	=	Strouhal number, $(=F^*A/U_\infty)$
t	=	time
U_{rms}	=	root mean square velocity
U_{rms}/U_∞	=	turbulence intensity
U_∞	=	freestream velocity
u	=	mean velocity
x	=	horizontal distance along the flat plate
x_{tran}	=	transition point
y	=	vertical distance above the flat plate
$\Delta\delta$	=	increase in boundary-layer thickness
δ	=	boundary-layer thickness
ν	=	kinematic viscosity of air
ω	=	angular velocity

I. Introduction

SINCE the introduction of the boundary-layer concept by Prandtl, there has been a constant challenge faced by scientists and engineers to minimize its adverse effects and control it to their advantage. A main objective of a control procedure is to prevent or at least delay the separation of the boundary layer from the wall. Methods employing suction, blowing, vortex generators, turbulence promoters, etc., have been investigated and applied extensively with a varying degree of success. However, the use of a moving or oscillating wall for boundary-layer control has received relatively little attention and there are many unanswered questions associated with the effects of oscillation on the boundary-layer development, especially under the presence of adverse pressure gradients. A moving surface attempts to accomplish this in two ways: 1) it retards the growth of the boundary layer by minimizing the relative motion between the surface and the freestream; 2) it adds momentum into the existing boundary layer.

Boundary-layer control by a moving surface was first demonstrated by Favre [1]. Favre ran an endless belt forming a portion of the upper surface of an aerofoil and delayed separation until high angles of attack. Since that initial study, boundary-layer control by surface motion has been examined and successfully demonstrated in a number of similar applications [2,3]. In those studies, however, the moving wall effects on the boundary layer itself have not been thoroughly examined.

For flows over moving walls, the point or line of vanishing wall shear does not necessarily coincide with separation, and this greatly complicates the problem. This was first observed by Rott [4] while analyzing the unsteady flow in the vicinity of a stagnation point. He observed that, although the wall shear vanished with an accompanying reverse flow, there was no singularity or breakdown of the boundary-layer assumptions. In seeking a generalized model for separation, Sears [5] postulated that the unsteady separation point is characterized by the simultaneous vanishing of the shear and the velocity at a point within the boundary later as seen by an observer moving with the velocity of the separation point. Moore [6], while investigating a steady flow over a moving wall, arrived at the same model for unsteady separation. On the basis of an intuitive relationship between steady flow over a moving wall and unsteady flow over a fixed wall, Moore was able to sketch the expected velocity profiles for both cases. He considered the possibility that a Goldstein-type singularity occurred at the location where the velocity profile simultaneously had zero velocity and a shear at a

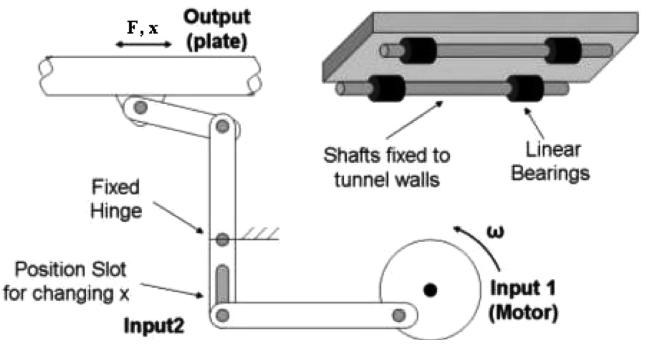

Fig. 1 Schematic of oscillation mechanism.

Received 26 May 2006; revision received 6 December 2006; accepted for publication 11 December 2006.

*Associate Professor (Senior Lecturer) of Aerodynamics and Ground Testing, Special Interest Group and Laboratory Head, School of Mechanical, Aerospace and Civil Engineering, Aero-Physics and Advanced Measurement Technology Laboratory. Member AIAA.

†Research Student, School of Mechanical, Aerospace and Civil Engineering, Aero-Physics and Advanced Measurement Technology Laboratory.

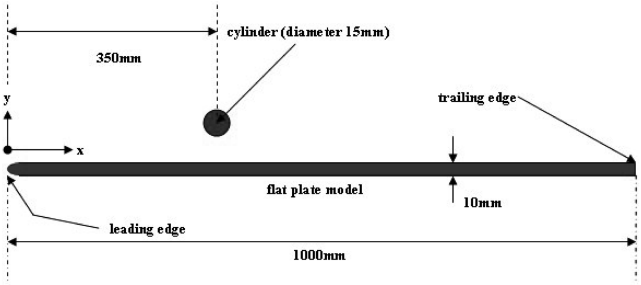

Fig. 2 Schematic of the experimental layout.

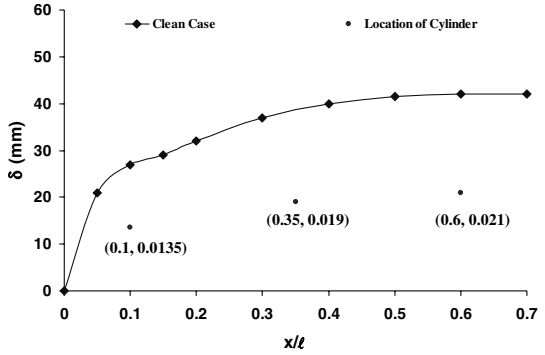

Fig. 3 Boundary-layer thickness for the clean case and cylinder location.

point above the moving wall. Equivalently, for unsteady separation on a fixed wall, the separation point was the location at which both the shear and the velocity vanished in a singular fashion in a frame of reference moving with the separation point. The main drawback of this Moore–Rott–Sears (MRS) model in the fixed wall case was the speed of the separation of the point known as a priori, making it difficult to locate this point and forcing researchers to rely on more qualitative measures for unsteady separation.

Moving walls have recently been employed by Bott and Bradshaw [7] to study the effect of high freestream turbulence on boundary layers as well as by Uzkan and Reynolds [8], Thomas and Hancock [9], and Aronson et al. [10] to study the interaction of turbulence with a wall. In these studies, however, the incident boundary layer was removed and no upstream induced velocity defect existed over the moving wall. When the wall speed equalled the freestream speed, a shear-free boundary layer developed on the moving wall. Because of

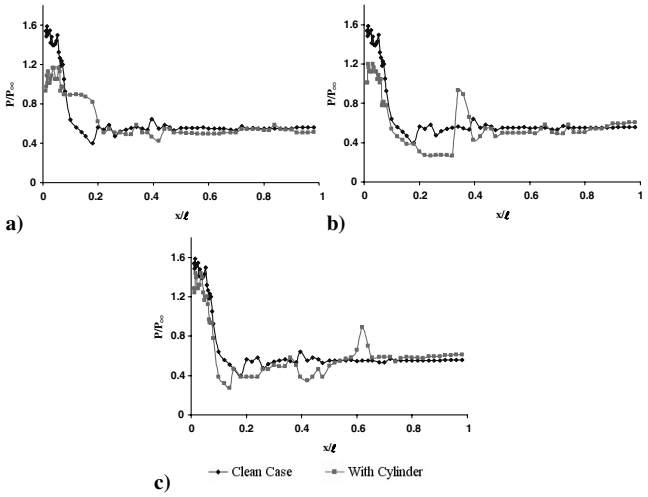

Fig. 4 Effect of cylinder on the pressure distribution along the flat plate model (stationary case); a) region I ($x/\ell = 0.10$); b) region II ($x/\ell = 0.35$); and c) region III ($x/\ell = 0.60$).

Table 1 Summary of cases tested with oscillation

A, m	F, Hz	S_t
0.005	2	0.0006
	4	0.0013
	6	0.0019
0.03	2	0.0038
	4	0.0075
	6	0.0113

Table 2 Horizontal and vertical locations of a cylinder

Region	x/ℓ	δ, mm	y, mm	(y/δ)
I	0.1	27	13.5	0.5
II	0.35	38	19	0.5
II	0.6	42	21	0.5

their importance as a means of improving near-wall turbulence models, such shear-free boundary layers have been studied theoretically by Hunt and Graham [11] as well as computationally by Perot and Moin [12].

A recent appraisal of the effects of wall oscillation on turbulent flows has been published by Karniadakis and Choi [13], where connection is made with drag reduction techniques, such as the excitation of the near-wall flow by transverse traveling waves [14]. Choi et al. [15] measured the streamwise variation of wall-shear stress over an oscillating plate in the turbulent boundary layer, showing that the skin-friction coefficient is reduced by as much as 45% over the oscillating wall as compared to that over the stationary wall. Choi and Clayton [16] proposed a mechanism of turbulent drag reduction based on the hot-wire anemometry and the flow visualization study of the near-wall turbulence structure over the oscillating wall, suggesting that a negative spanwise vorticity that is generated at the edge of the viscous sublayer plays a significant role in reducing the skin-friction drag of the turbulent boundary layer.

The objectives of the present study are 1) to examine in detail the effects of flat plate oscillation (in the x direction) on the boundary-layer development under the presence of adverse pressure gradients; and 2) to complement the existing database on moving walls at subsonic speeds for computational fluid dynamics (CFD) code validation and next generation design tool development.

II. Experimental Setup and Apparatus

The experiments were conducted in a low speed subsonic wind tunnel. The tunnel has a test section of 1.4 (length) × 0.45 (width) × 0.45 m (height). The ceiling and side walls are made of high transparency perspex to allow optical access. The contraction ratio of the nozzle is 6.5 to 1 and the maximum velocity of the test section is

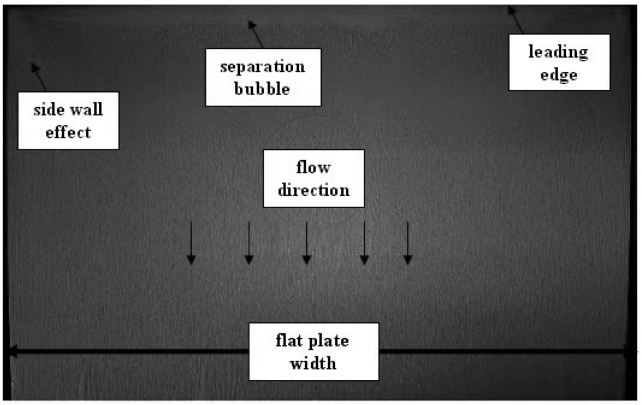

Fig. 5 Oil flow visualization on the flat plate model (clean case, stationary).

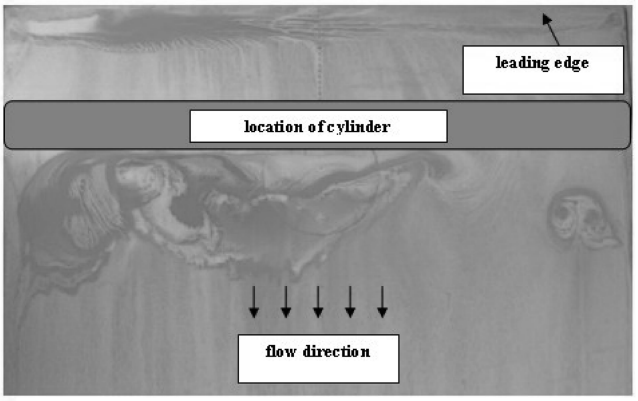

a)

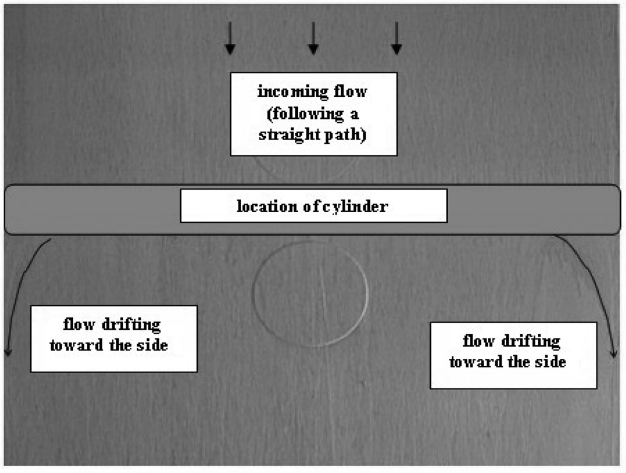

b)

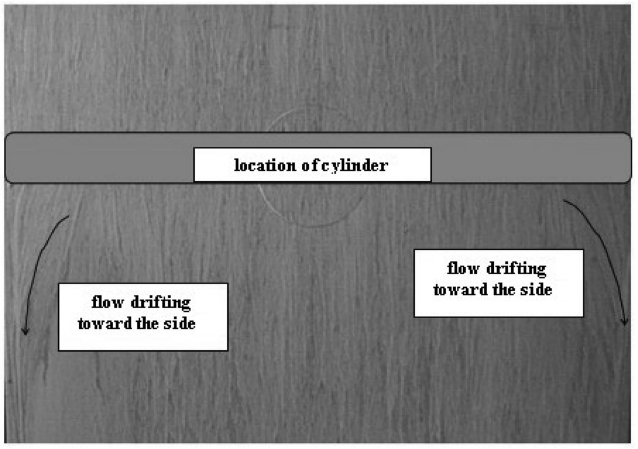

c)

Fig. 6 a) Oil flow visualization with the cylinder placed at $x/\ell = 0.10$ (region I). b) Oil flow visualization with the cylinder placed at $x/\ell = 0.35$ (region II). c) Oil flow visualization with the cylinder placed at $x/\ell = 0.60$ (region III).

32 m/s. The freestream turbulent intensity of the tunnel is less than 0.15%. All measurements were taken at a freestream velocity of 16 m/s. The experiments were performed at a Re_N equal to 10^6 based on the plate chord length. A 1 m-long flat plate made of aluminum was used, with its width covering the entire test section, placed 0.16 m above the floor of the test section. Its surface had a smooth finish. It was placed on linear bearing rods, to minimize friction and ensure its oscillation in the x (streamwise) direction. Figure 1 shows the oscillation mechanism (installed underneath the wind tunnel working section) with the flat plate model attached on

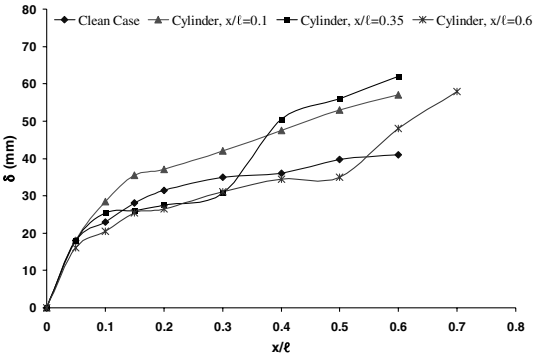

Fig. 7 Effects of the cylinder on boundary-layer thickness (stationary case).

the top. The whole system was rested on a heavy metal base plate to avoid unwanted vibrations at higher frequencies of operation. The flat plate model was made to oscillate at a range of frequencies 0–6 Hz and amplitudes 0–0.03 m. Table 1 summarizes the cases tested with oscillation.

To produce the effects of adverse pressure gradients on the flow over the flat plate, a circular cylinder was placed at various locations over the flat plate within the boundary layer. The Reynolds number of the cylinder was 16,000 based on its diameter of 0.015 m and the freestream velocity of 16 m/s. In all cases, the $y/\delta = 0.5$ was kept constant. The chosen experimental setup, including Reynolds number, reduced frequencies of oscillation, and pressure gradients, aims to provide 1) a better understanding of the fundamental aspects of the boundary-layer behavior under these conditions; and 2) data for validation of the CFD study conducted in parallel by the sponsors of the project.

Sixty-five pressure tapings connected to high sensitivity pressure transducers were placed along the centerline of the plate at a distance of 0.02 m from each other. The diameter of each taping was 0.001 m. Boundary-layer surveys were performed with a single probe TSI hot-wire system. The hot-wire probe was mounted on the top of the wind tunnel and it was placed into the test section via a slot in the ceiling of the test section. Attached to the probe was a traverse device which moved the probe to the desired location along the flat plate. A microgauge was connected to this system to monitor the vertical distance of the hot wire from the flat plate surface during the measurements. The data from the pressure transducers and the hot-wire probe were captured using a data acquisition system with LabVIEW 7.1 software. Data were recorded over a period of 2 s at a sampling rate of 1 kHz. The accuracy for the pressure measurements was $\pm 3.5\%$. A static calibration of the hot wire, based on King's law, was obtained by placing the probe in the freestream at the start of the working section. The instrument uncertainty in the velocity measurements was found to be $\pm 2.5\%$.

For the oil flow visualization measurements, the model was painted with a mixture of titanium oxide, paraffin, and fluorescent paint. Pictures were then taken using a digital camera. Figure 2 shows the schematic of the experimental layout.

III. Results and Discussion

A. Case A: No Oscillation

1. Pressure Measurements

Table 2 shows the location of the cylinder placed at different regions along the flat plate. Figure 3 depicts the boundary-layer thickness for the clean case and cylinder locations in regions I, II, and III. The x and y coordinates of the center location of the cylinder are given in Fig. 3.

Figure 4 shows the pressure distributions with the cylinder placed in regions I ($x/\ell = 0.10$), II ($x/\ell = 0.35$), and III ($x/\ell = 0.60$). When the cylinder is placed in region I, Fig. 4a (near the leading edge of the flat plate and downstream of the separation bubble), the upstream surface pressures are significantly reduced. Behind the cylinder, an increase in surface pressures is observed, which recovers

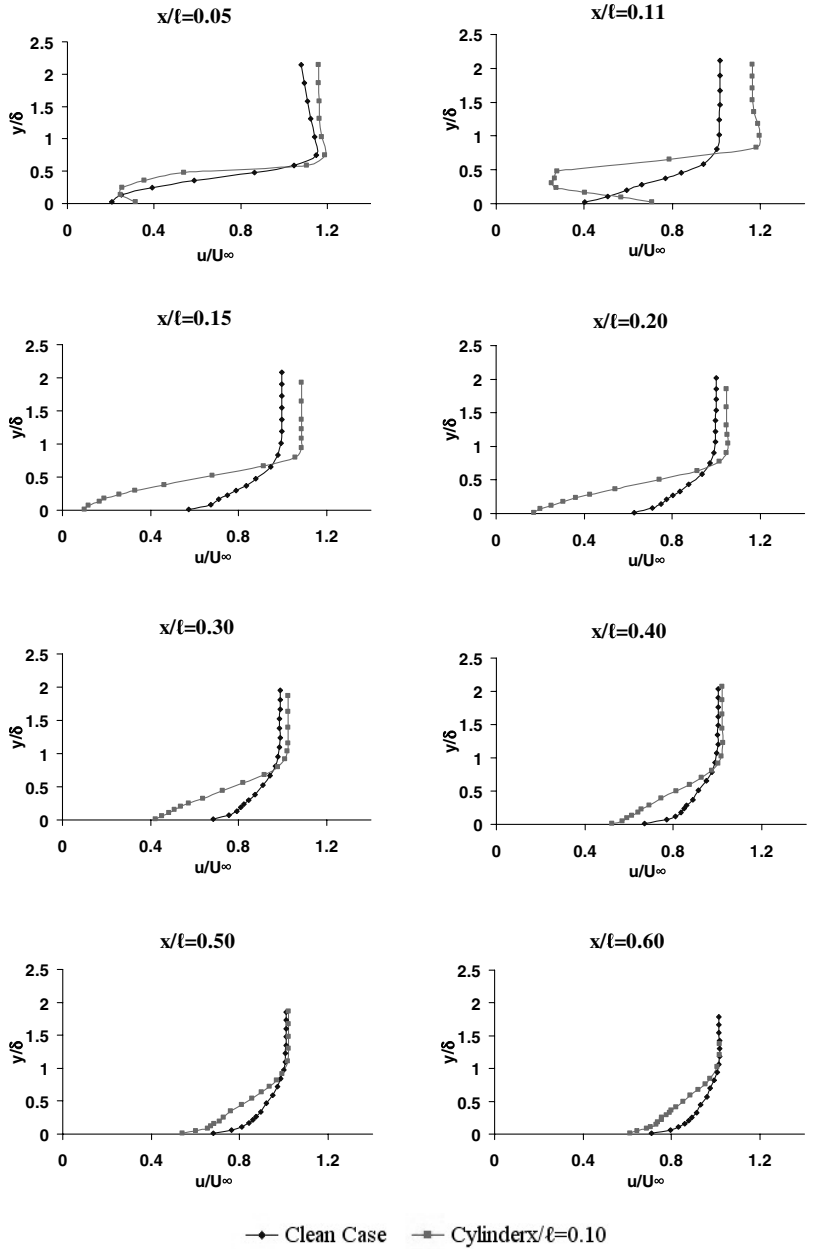

Fig. 8 Effects of the cylinder ($x/\ell = 0.10$) on the mean velocity profiles (stationary case).

back to the clean case levels. Downstream of the latter location, the pressure on the flat plate surface seems to be unaffected due to the presence of the cylinder.

Figure 4b shows that the presence of the cylinder affects the leading edge causing a reduction in pressure; however, this effect is less pronounced compared to the region I case, Fig. 4a. Reduced pressures on the flat plate surface are observed ahead of the cylinder, which then rise to a peak. The flow (on the surface of the flat plate) stagnates in the region below the cylinder. This is also supported by the boundary-layer surveys and oil flow visualization measurements. The pressure drops again behind the cylinder, which recovers back to the clean case levels. The region affected by the presence of the cylinder extends up to $x/\ell = 0.45$. Figure 4c shows that with the cylinder placed at $x/\ell = 0.60$, the region close to the leading edge of the flat plate remains unaffected. Reduced pressures are recorded upstream of the cylinder reaching a peak that exists at $x/\ell = 0.60$. The pressure then recovers immediately back to the clean case levels. The pressure peak is smaller than that of the region II case, Fig. 4b. In summary, the effect of the presence of the cylinder is more pronounced in the region II case. For the region I case, its effect is restricted in the leading edge region, whereas for the region III case, the boundary layer is more robust and its effect is considerably less pronounced.

2. *Oil Flow Visualization*

Figure 5 shows the surface flow for the clean case. The flow separates very near the rounded leading edge causing the formation of separation bubble. The flow reattaches after approximately 0.05 m. The side wall effects are also captured on either side of the plate. The presence of the separation bubble forces transition to occur earlier, causing the thickening of the boundary layer (see also Secs. I and III). Figure 3 shows the dramatic and continuous increase in the boundary thickness after the separation bubble which reaches a plateau after $x/\ell = 0.45$. Theory predicted the transition point at 0.23 m from the leading edge using the following equation:

$$x_{\text{tran}} = \frac{Re_{\text{crit}} \cdot \nu}{U_\infty}$$

A critical Reynolds number of 5×10^5 was employed. In the present experiment, the boundary in region I is transitional. In

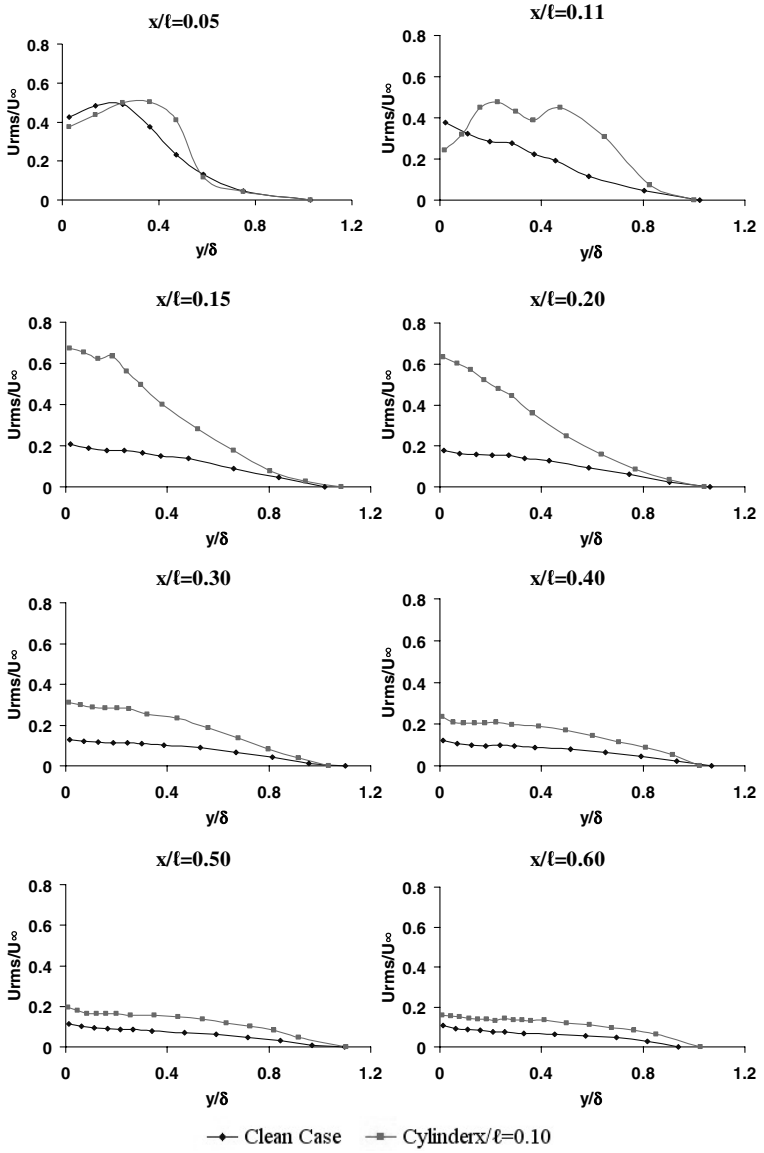

Fig. 9 Effects of the cylinder ($x/\ell = 0.10$) on the turbulence intensity profiles (stationary case).

region III, the boundary layer is turbulent (fully developed), whereas in region II, the boundary layer is still at the late stages of its transition to turbulence.

Figure 6a shows the oil flow visualization with the cylinder placed in region I. The pattern is complicated due to the proximity of the cylinder to the separation bubble. Ahead of the cylinder, the surface flow is distorted and the separation bubble is no longer symmetrical in shape. The separation bubble interacts with the cylinder, which causes the separated flow from the surface to form a strong wake which is highly unstable. This wake eventually rolls into discrete vortices (possibly forming a Karman vortex street) which interact with the flat plate behind the cylinder. The surface flow recovers back to the clean case after approximately 1.5 cylinder diameters. Figure 6b shows that by placing the cylinder in region II, the flow tends to drift toward the sides of the plate downstream of the cylinder for a short distance and then recovers again.

Figure 6c shows that by placing the cylinder in region III, the effect is similar to that observed in the region II case. The flow seems to be undisturbed in the central region of the plate, whereas on the sides, the fluid is drawn toward it. The flow then recovers again as it moves toward the trailing edge. The distance during which the flow tends to drift toward the sides is related to the distance over which there is a sudden increase in static pressure on the flat plate due to the cylinder placed either in regions II or III, see Figs. 4b and 4c.

3. Boundary-Layer Measurements

Boundary-layer measurements were conducted along the plate centerline. Figure 7 shows the boundary-layer thickness (δ) distributions for the flat plate with and without the cylinder. It can be seen that the effect of the cylinder is to make the boundary layer thicker as the flow decelerates due to the increasing surface pressure. The adverse effects of the cylinder on the flow are more pronounced for the region II ($x/\ell = 0.35$) case as it causes the largest and more steep increase in δ.

Figures 8 and 9 show the effects of the cylinder placed in region I on the mean velocity and turbulence intensity profiles along the flat plate. The deceleration effect on the velocity profiles due to the cylinder is evident from Fig. 8. This effect is getting smaller further downstream. At $x/\ell = 0.05$ and 0.11, the velocity close to the wall for the clean case is lower than the velocity with the cylinder in place, which is due to the mutual interaction between the cylinder and the separation bubble. This is also supported from the pressure measurements, Fig. 4a, where the upstream surface pressures are reduced, whereas behind the cylinder the surface pressures are increased. This effect is then reversed at successive locations downstream of the flat plate where the velocities close to the wall for the clean case are always higher than those with the cylinder in place. The largest velocity difference near the wall region between the two cases is observed at $x/\ell = 0.15$. This difference gets smaller at

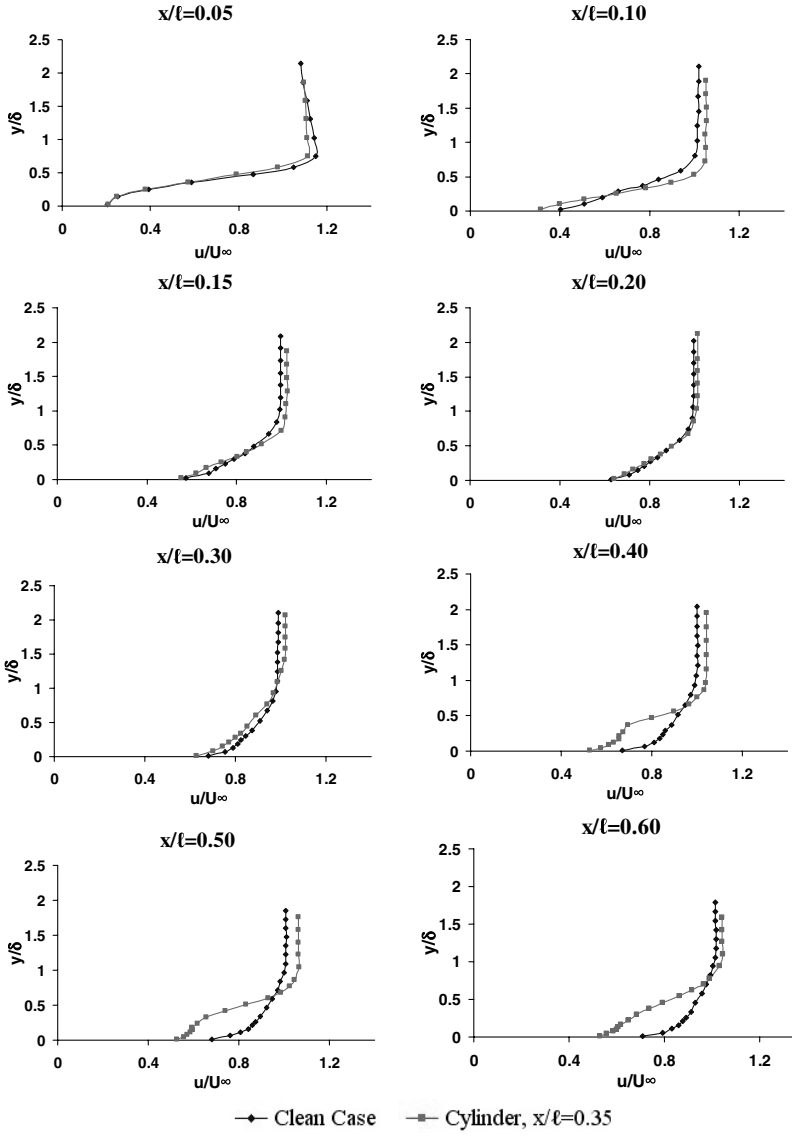

Fig. 10 Effects of the cylinder ($x/\ell = 0.35$) on the mean velocity profiles (stationary case).

different locations further downstream. The presence of the cylinder alters the shape of the velocity profiles and its effect is felt throughout the plate.

The presence of the cylinder causes an increase on the turbulent intensities for all positions, Fig. 9; however, the increase is more dramatic up to $x/\ell = 0.30$, due to the strong highly unstable wake which interacts with the flat plate. After $x/\ell = 0.30$, the increase is getting smaller and turbulence intensity reaches levels close to the clean case, which shows that the wake structures eventually dissipate. The highest increase in turbulence levels is observed at $x/\ell = 0.15$ and $x/\ell = 0.20$. For example, at $x/\ell = 0.15$, the turbulence intensity near the wall region increases from 0.2 to 0.65, whereas at $x/\ell = 0.60$, an increase of 0.05 is observed. These results correlate with the velocity profiles shown in Fig. 8.

Figures 10 and 11 show the effect of the cylinder placed in region II on the mean velocity and turbulence intensity profiles along the flat plate. The upstream deceleration effect due to the cylinder is small, whereas downstream its effect is more pronounced, Fig. 10, causing the velocity profiles to become less full. Further downstream, the boundary layer shows signs of recovery. At distances greater than $x/\ell = 0.30$, the velocity defect in the wake of the cylinder occupies a larger portion of the boundary layer and this results in an increase in δ compared with the clean case as seen in Fig. 7.

Figure 11 shows an increase in turbulence intensity levels due to the cylinder being placed in region II. In the immediate upstream region, the effect of the cylinder is small; however, at locations behind it, high levels of turbulence were recorded. It is worth noting that the presence of the cylinder causes an increase in turbulence intensity levels near the leading edge region. Its effect is also evident in the pressure measurements, Fig. 4b, as was discussed in Sec. I. With the cylinder placed at $x/\ell = 0.10$, the highest increase in turbulence intensity in the leading edge region was 0.45, whereas with the cylinder placed at $x/\ell = 0.35$, the increase in turbulence intensity reduces to 0.15. This reduction in turbulence levels indicates the importance of the height of the cylinder above the flat plate. Hence by placing the cylinder closer to the flat plate (region I case), its effects on the turbulence levels are higher than those when it is placed farther away (region II case).

Figures 12 and 13 show the velocity and turbulence intensity profiles with the cylinder placed in region III. Just behind the cylinder, the velocity profiles show that the flow accelerates near the wall region but then decelerates abruptly, Fig. 12. This is due to the wake formed behind the cylinder which causes the decrease in momentum inside the boundary layer. The deceleration effect gets smaller at $x/\ell = 0.70$. At this location, the velocity near the wall region for the clean case is smaller than that with the cylinder. It is between these two locations, that δ increases dramatically, Fig. 7. Behind the cylinder, there is an increase in the turbulence intensity levels. The peak in Fig. 13 at $x/\ell = 0.60$ corresponds to the vertical location of the cylinder and it is associated with its wake. As the hot-wire probe is traversed away from the cylinder, the turbulence level

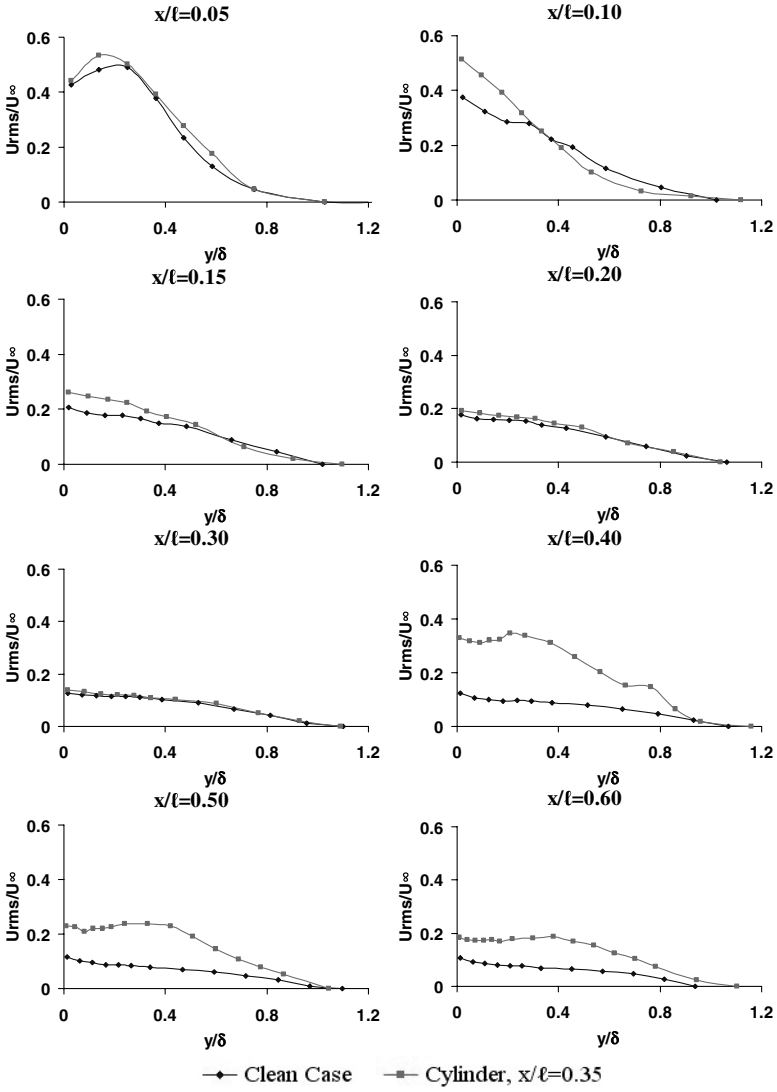

Fig. 11 Effects of the cylinder ($x/\ell = 0.35$) on the turbulent intensity profiles (stationary case).

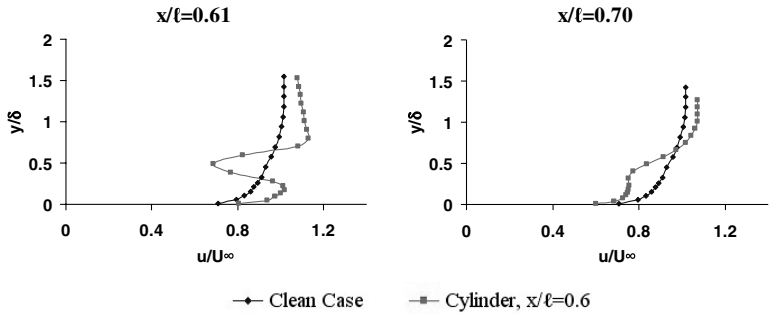

Fig. 12 Effects of the cylinder ($x/\ell = 0.60$) on the mean velocity profiles (stationary case).

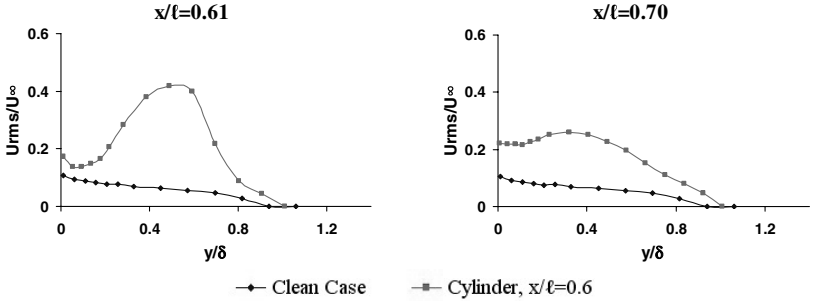

Fig. 13 Effects of the cylinder ($x/\ell = 0.60$) on the turbulent intensity profiles (stationary case).

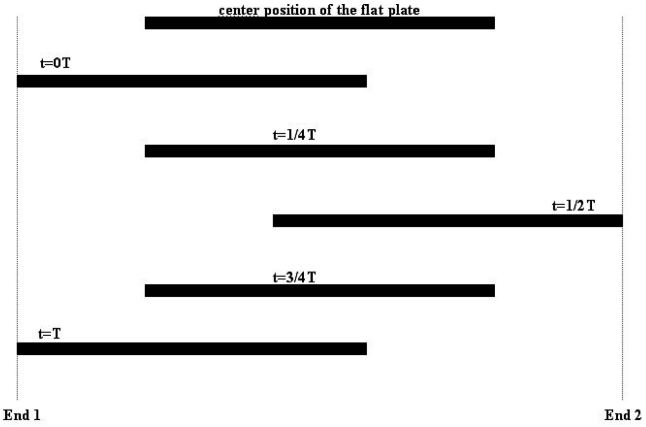

Fig. 14 Flat plate undergoing one complete oscillation cycle.

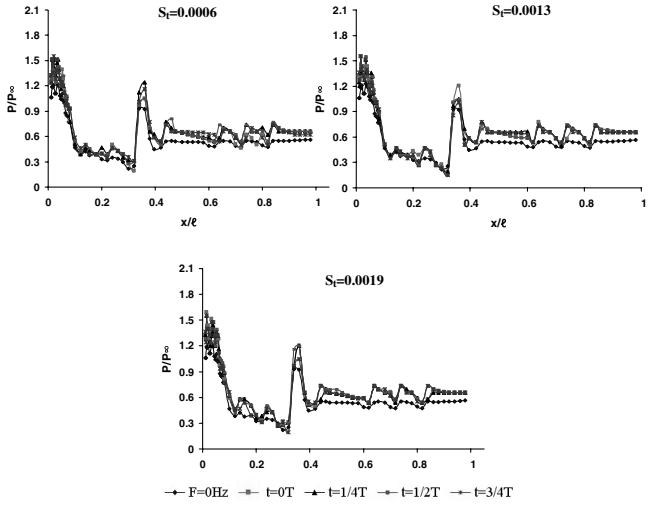

Fig. 15 Effects of oscillation at $A = 0.005$ m with the cylinder placed at $x/\ell = 0.35$.

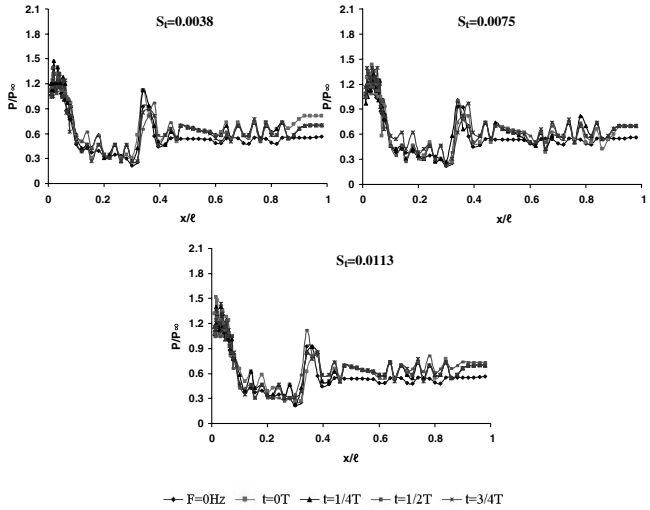

Fig. 16 Effects of oscillation at $A = 0.03$ m with the cylinder placed at $x/\ell = 0.35$.

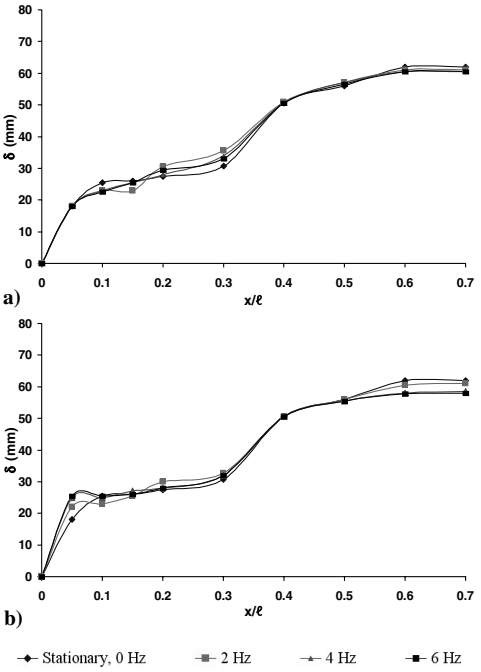

Fig. 17 Effects of oscillation at $A = 0.005$ m and 0.03 m on the boundary-layer thickness with the cylinder placed at $x/\ell = 0.35$; (a) $A = 0.005$ m; (b) $A = 0.03$ m.

drops. At a distance of $y/\delta = 1.0$, that is, at the boundary-layer edge, the turbulence intensities for the two cases are the same.

B. Case B: With Oscillation

1. Pressure Measurements

Figure 14 shows a graphical representation of the movement of the flat plate model when it undergoes one complete oscillation cycle. One complete oscillation cycle of the flat plate is divided into four phases. $t = 0T$ represents the beginning of the measurements, $t = 1/4T$ represents the point at which the plate has completed $1/4$th of its oscillation cycle. $t = 3/4T$ represents the point at which the plate has completed $3/4$th of its oscillation cycle and $t = T$ represents the point at which the flat plate has completed one oscillation cycle. The pressure at $t = T$ would be the same as that at $t = 0T$. The plate was allowed to oscillate for 4 s in all cases and the data were captured. The pressure at any given point within an oscillation cycle was deduced from the data recorded. A triggering mechanism was designed and placed in the wind tunnel to ensure consistency in the data and a known and common starting point for all measurements in the oscillation cycle.

The effects of oscillation were examined in the presence of a cylinder placed in region II of the flow. Figure 15 shows the effects oscillation at amplitude equal to 0.005 m. Increased levels of pressure can be seen on the entire length of the plate. The oscillation of pressures near the leading edge is associated with the separation bubble. The pressure peak that exists between $x/\ell = 0.3$ and 0.4 increases in magnitude due to oscillation. However, at different points during the oscillation cycle, the peak also varies in magnitude. Behind the cylinder, there is a continuous rise in pressure up to the trailing edge of the plate. The effects due to the frequency of oscillation can be mainly seen at the pressure peak point. At 2 Hz, the peak rises to the maximum, when the flat plate has completed $1/4$th of its oscillation cycle and it is moving against the direction of the incoming flow. At 4 Hz, the peak rises to the maximum at $t = 0T$, the point at which the flat plate starts its oscillation cycle. At this point the flat plate is moving in the direction of the flow. However, at 6 Hz, the peak rises to the maximum for the first three points of the oscillation cycle, that is, $t = 0T$, $t = 1/4T$ and $t = 1/2T$. At $t = 3/4T$, there is a decrease in the magnitude of the pressure peak but its value is still higher than that for the stationary case.

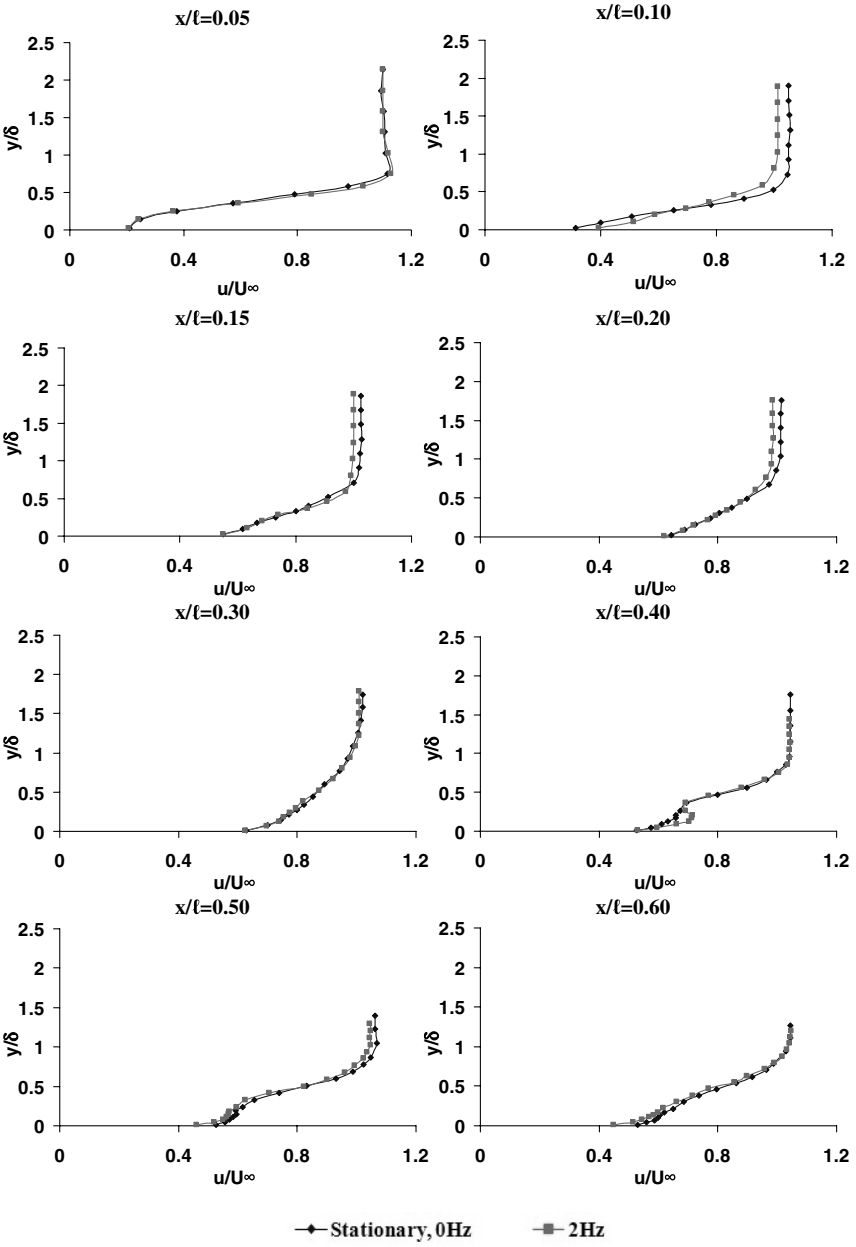

Fig. 18 Effects of oscillation at $S_t = 0.0006$ on the mean velocity profiles.

When the amplitude is increased to 0.03 m, Fig. 16, the effects due to oscillation are mainly seen behind the cylinder. The pressures near the leading edge still increase but the effects are smaller than those observed in Fig. 15. The displacement of the pressure peak from its mean position, $x/\ell = 0.35$, is the most obvious feature in Fig. 16. This happens because the stagnation point that exists on the surface of the flat plate moves due to the higher amplitude of oscillation relative to the position of the cylinder. The effect of frequency on the pressure peak is also evident from the pressure measurements. The highest effect seems to take place at a frequency of 2 Hz. At 4 Hz, even though the displacement of the peak is measured during the various stages of the oscillation cycle, the magnitude of the peak remains mainly unaffected. Behind the cylinder, as was seen for the lower amplitude case, the surface pressures increase up to the trailing edge of the flat plate. The data shown in Figs. 15 and 16 are representative of one time sample. The irregularities observed in the region between $x/\ell = 0.6$ to 0.85 are due to the differences in the tubing connected to the pressure taps.

2. *Boundary-Layer Measurements*

Figure 17 shows the effects of oscillation at amplitudes of 0.005 and 0.03 m on the mean boundary-layer thickness along the flat plate. Just ahead of the cylinder, the boundary-layer thickness seems to increase due to oscillation. However, with increasing frequency of oscillation, the effects are getting smaller. Downstream of the cylinder, the boundary layer remains unaffected due to oscillation. At higher amplitude, the boundary-layer thickness increases near the leading edge. At a distance of $x/\ell = 0.05$, with increasing frequency of oscillation, the boundary-layer thickness increases. Unlike the lower amplitude case, at $A = 0.03$ m, the boundary layer is affected downstream of the location of the cylinder. At a distance of $x/\ell = 0.6$, the effect of oscillation causes a decrease in δ.

Figure 18 shows the mean velocity profiles at an amplitude of 0.005 m and frequency of 2 Hz. At a distance of $x/\ell = 0.10$, the flow near the wall region is accelerated. The flow then decelerates at $y/\delta = 0.25$. The momentum of the flow reduces along the profile due to oscillation. The flow seems unaffected downstream of $x/\ell = 0.10$; however, some changes in the velocity profiles are seen behind the cylinder. At $x/\ell = 0.40$, a velocity overshoot is observed in the profile, starting at $y/\delta = 0.05$. At distances of $x/\ell = 0.50$ and 0.60, a decrease in velocity due to oscillation is seen near the wall region only. The results show that the velocity profiles are mainly affected just behind the cylinder when the plate oscillates at low amplitude.

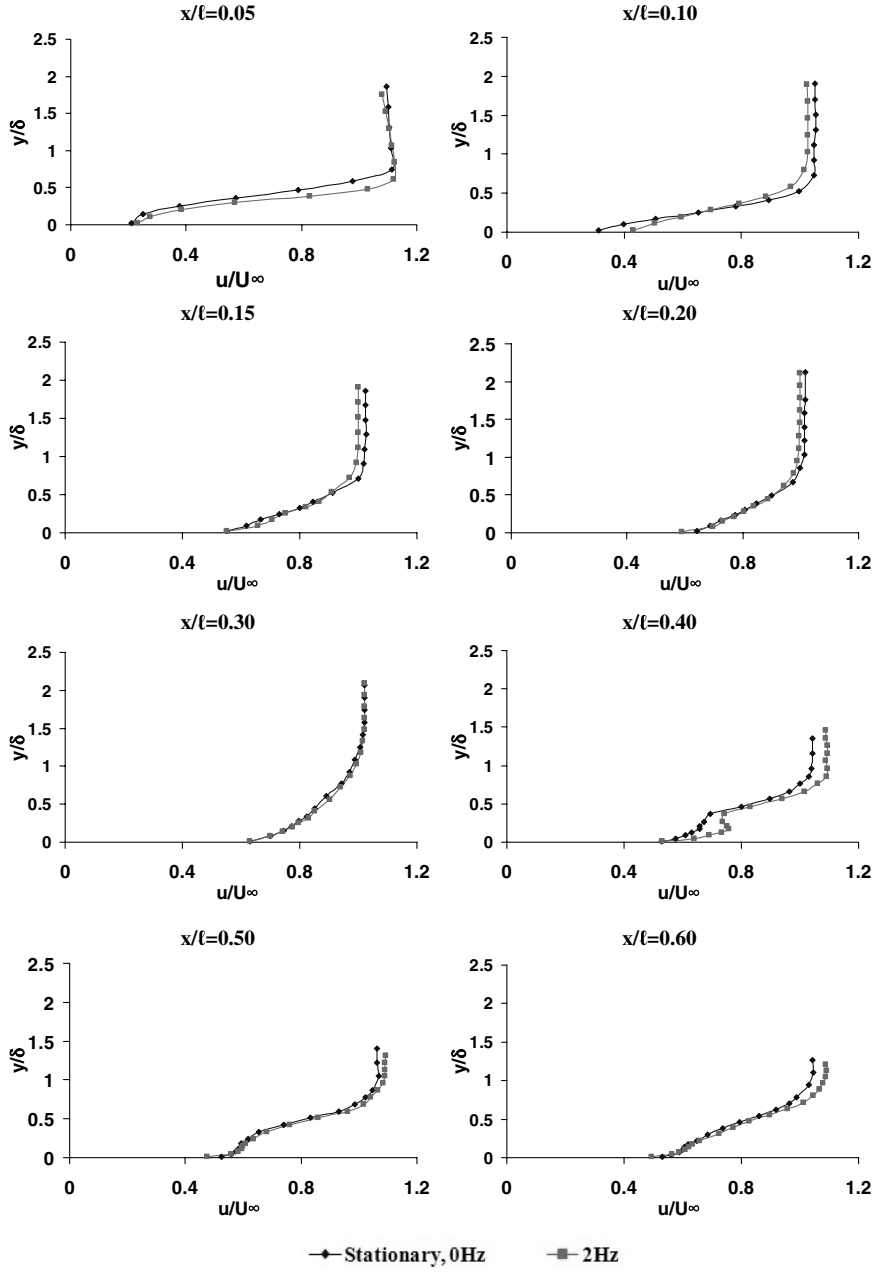

Fig. 19 Effects of oscillation at $S_t = 0.0038$ on the mean velocity profiles.

Figure 19 shows the mean velocity profiles when the amplitude of oscillation is increased to 0.03 m. Unlike the lower amplitude case, changes are observed in the profile at $x/\ell = 0.05$. The effect of oscillation at 2 Hz is to accelerate the flow near the wall region. The momentum of the flow is also larger along the profile than the stationary case. An accelerated flow near the wall region at $x/\ell = 0.10$ is also measured. Behind the cylinder, an overshoot in the velocity is also seen in the profile at $x/\ell = 0.40$. However, in this case, the velocity is higher than the stationary case.

Figures 20 and 21 show the effect of oscillation on turbulence intensity profiles. At $A = 0.005$ m, the turbulence levels are slightly lower than the stationary case in the upstream region of the cylinder, Fig. 20. Behind the cylinder, elevated levels of turbulence intensity are seen in the profiles. It is conjectured that the effect of oscillation increases the effect of the wake on the boundary layer behind the cylinder.

Increasing the amplitude of oscillation to 0.03 m causes the turbulence intensity near the wall in the upstream region of the cylinder to reduce. The effect is more pronounced near the leading edge, Fig. 21. Behind the cylinder, the changes in turbulence intensity levels are quite small compared to those measured at the low amplitude case.

Figure 22 shows the effect of oscillation at an amplitude equal to 0.03 m on the flow near the leading edge of the plate just behind the separation bubble. The figure depicts the voltage variation against time from the hot-wire probe and this was captured with the probe inside the boundary-layer edge. It can be seen from the stationary case, the graph is a straight line as expected, indicating that the flow is not oscillating. However, the graphs obtained by oscillating the plate exhibit the oscillatory behavior of the flow with the number of cycles increasing with increasing Strouhal number. The oscillation diminishes as the probe is traversed outside the boundary layer. This indicates that the oscillation is present only within the boundary layer. This effect occurred only in this region of the flow near the leading edge. Downstream of this location, that is, both in regions II and III such oscillation was not observed. It is conjectured that this is associated with the presence of the separation bubble and the influence that the flat plate oscillation may have on its structure, properties, and characteristics.

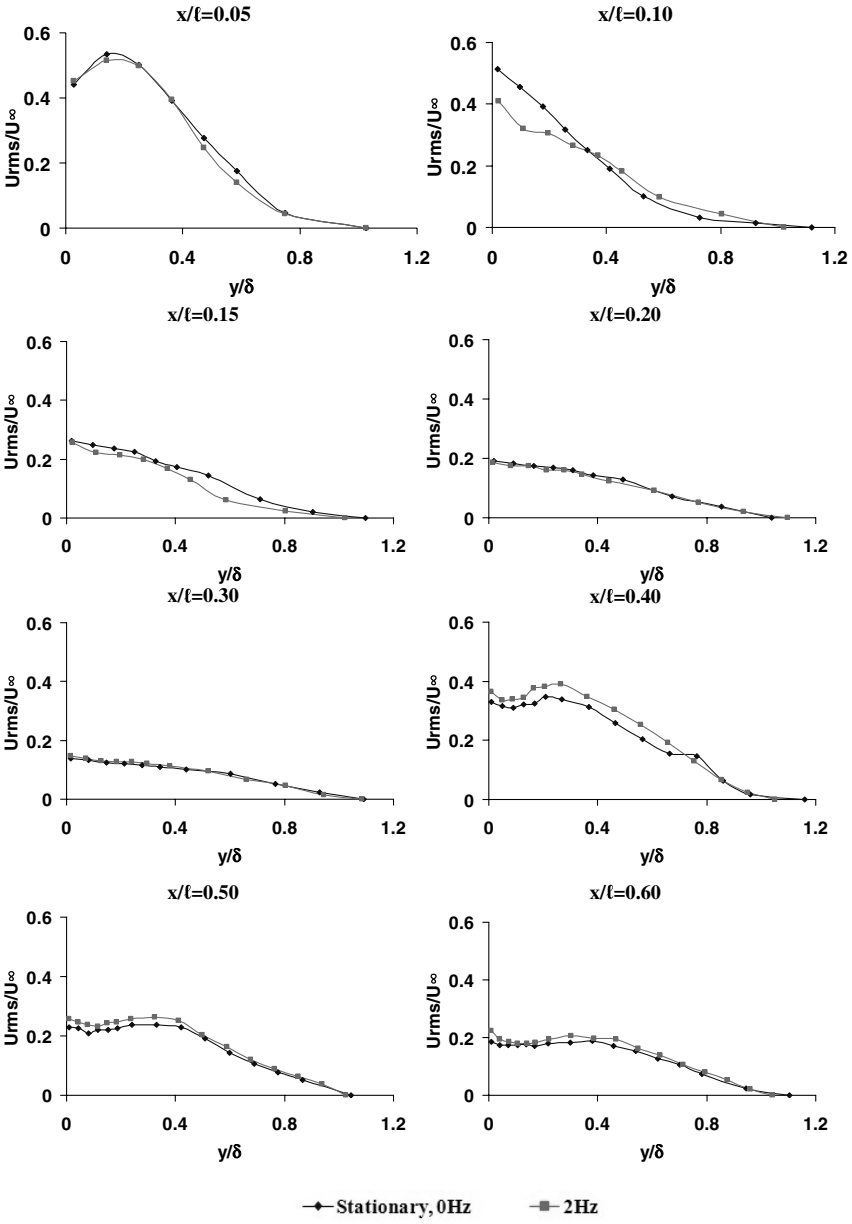

Fig. 20 Effects of oscillation at $S_t = 0.0006$ on the turbulence intensity profiles.

IV. Conclusions

The flow separates very near the rounded leading edge causing the formation of a separation bubble. The presence of the separation bubble forces transition, causing the thickening of the boundary layer. The cylinder causes a reduction in the upstream surface pressures and an increase in the downstream pressures which recover back to the clean case levels. The effect of the presence of the cylinder is more pronounced in the region II case. For the region I case, its effect is restricted in the leading edge region, whereas for the region III case, the boundary layer is more robust and the effect of the cylinder is considerably less pronounced. In the region I case, the flowfield is complicated due to the proximity of the cylinder to the separation bubble. A strong wake is formed behind the cylinder which interacts with the boundary layer. Both velocity and turbulence intensity profiles are affected for all positions tested. The reduction in turbulence levels near the leading edge region indicates the importance of the height of the cylinder above the flat plate. By placing the cylinder closer to the flat plate (region I case), its effects on the turbulence levels are higher than those when it is placed further away (region II and III cases).

Oscillation causes increased levels of pressure on the entire length of the plate. The pressure peak in the cylinder region increases in magnitude due to oscillation. During an oscillation cycle, the peak also varies in magnitude. With increasing Strouhal number, a displacement of the pressure peak from its mean position occurs. The strongest effect seems to take place at $S_t = 0.0038$. Just ahead of the cylinder, the boundary-layer thickness increases due to oscillation. However, with increasing S_t, the effects are getting smaller. Unlike the lower amplitude case, at $A = 0.03$ m, the boundary layer is affected downstream of the location of the cylinder causing a decrease in δ. Oscillation increases the effect of the wake of the cylinder on the boundary-layer properties behind the cylinder. The flow in the leading edge region exhibits an oscillatory behavior with the number of cycles increasing with increasing Strouhal number. This may be associated with the presence of the separation bubble and the influence that the flat plate oscillation may have on its structure, properties, and characteristics. Further studies are under away to clarify these effects and examine in detail the flow physics. Further experiments are also being carried out to examine the effect of oscillation at range amplitudes and frequencies with the cylinder

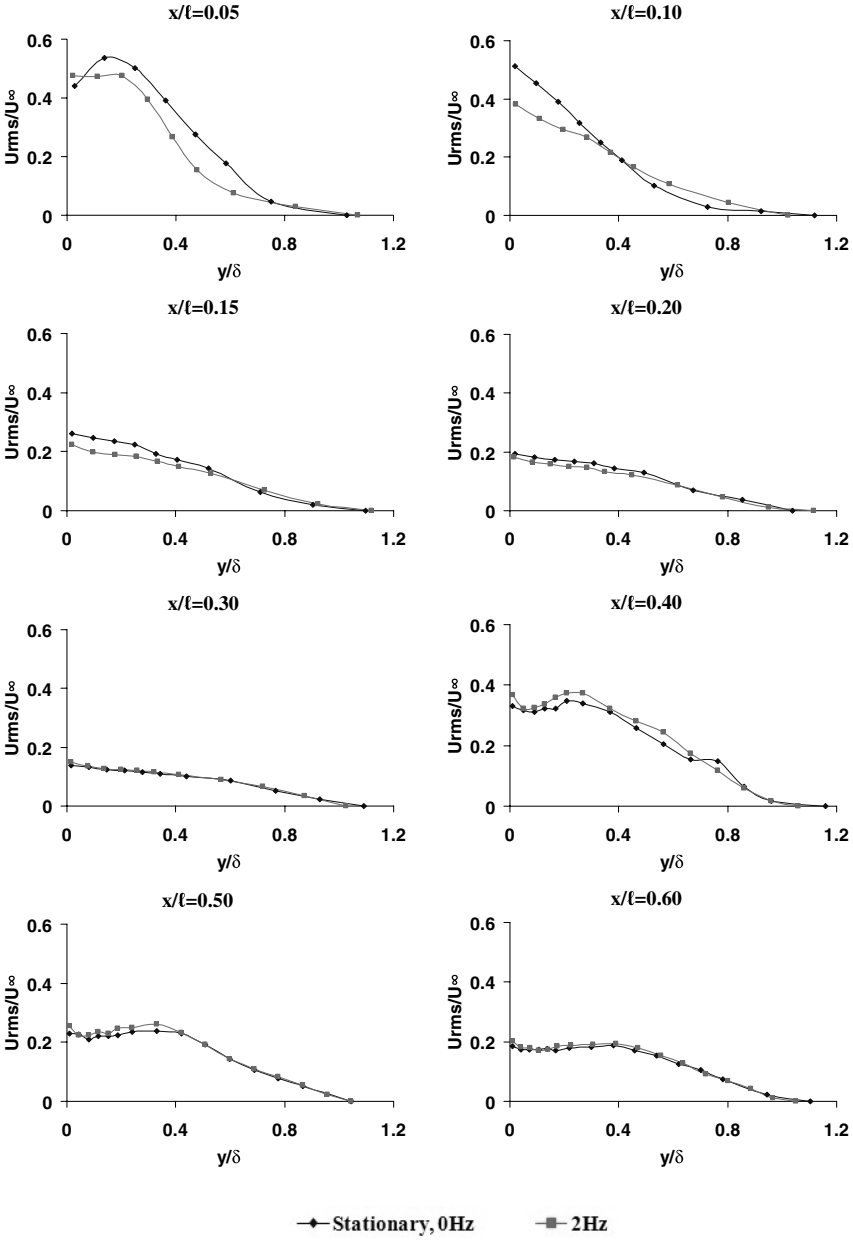

Fig. 21 Effects of oscillation at $S_t = 0.0038$ on the turbulence intensity profiles.

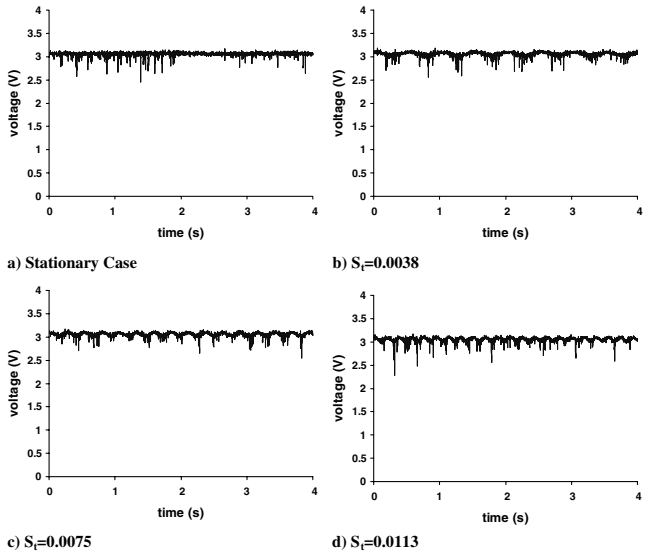

Fig. 22 Effects of oscillation on the flow near the leading edge region.

placed within different regions of the flow in the presence and absence of favorable pressure gradients.

Acknowledgements

The authors would like to thank ORS for their financial support and Neel Shah for his assistance in the investigation.

References

[1] Favre, A., "Contribution a L'etude Experimentale Des Mouvements Hydrodynamques a Deux Dimensions," Ph.D. Thesis, University of Paris, France, 1938.

[2] Modi, V. J., Fernando, M. S. U. K., and Yokomiz, T., "Moving Surface Boundary-Layer Control: Studies with Bluff Bodies and Application," *AIAA Journal*, Vol. 29, No. 2, 1991, pp. 1400–1406.

[3] Modi, V. J., "Moving Surface Boundary Layer Control: A Review," *Journal of Fluids and Structures*, Vol. 11, No. 4, 1997, pp. 627–663.

[4] Rott, N., "Unsteady Viscous Flow in the Vicinity of Stagnation Point," *Quarterly of Applied Mathematics*, Vol. 13, Sept. 1956, pp. 444–451.

[5] Sears, W. R., "Some Recent Developments in Airfoil Theory," *Journal of Aeronautical Science*, Vol. 23, May 1956, pp. 490–499.

[6] Moore, F. K., "On the Separation of the Unsteady Laminar Boundary Layer," *Boundary Layer Research*, edited by H. Gortler, Springer–

Verlag, Berlin, 1958, pp. 296–310.
[7] Bott, D. M., and Bradshaw, P., "Effect of High Freestream Turbulence on Boundary-Layer Skin Friction and Heat Transfer," Mechanical Engineering Department, Stanford University, Rept. MD-75, 1997.
[8] Uzkan, T., and Reynolds, W. C., "A Shear-Free Turbulent Boundary Layer," *Journal of Fluid Mechanics*, Vol. 28, Aug. 1967, pp. 803–821.
[9] Thomas, N. H., and Hancock, P. E., "Grid Turbulence Near a Moving Wall," *Journal of Fluid Mechanics*, Vol. 82, June 1977, pp. 481–496.
[10] Aronson, D., Johannson, A. V., and Lofdahl, L., "Shear Free Turbulence Near a Wall," *Journal of Fluid Mechanics*, Vol. 338, March 1997, pp. 363–385.
[11] Hunt, J. C. R., and Graham, J. M. R., "Free Stream Turbulence Near Plane Boundaries," *Journal of Fluid Mechanics*, Vol. 84, Aug. 1978, pp. 209–235.
[12] Perot, J. B., and Moin, P., "Shear Free Turbulent Boundary Layers," *Journal of Fluid Mechanics*, Vol. 295, Dec. 1995, pp. 199–227.
[13] Karniadakis, G. E., and Choi, K. S., "Mechanisms on Transverse Motions in Turbulent Wall Flows," *Annual Review of Fluid Mechanics*, Vol. 35, June 2003, pp. 45–62.
[14] Du, Y., Symeonidis, V., and Karniadakis, G. E., "Drag Reduction in Wall bounded Turbulence via a Transverse Travelling Wave," *Journal of Fluid Mechanics*, Vol. 457, May 2002, pp. 1–34.
[15] Choi, K. S., DeBisschop, J. R., and Clayton, B. R., "Turbulent Boundary Layer Control by Means of Spanwise-Wall Oscillation," *AIAA Journal*, Vol. 36, No. 7, 1998, pp. 1157–1163.
[16] Choi, K. S., and Clayton, B. R., "The Mechanism of Turbulent Drag Reduction with Wall Oscillation," *International Journal of Heat Fluid Flow*, Vol. 22, No. 3, 2001, pp. 1–9.